World Scientific
www.worldscientific.com

JAPAN SOCIETY OF CIVIL ENGINEERS
COASTAL ENGINEERING COMMITTEE

Coastal Engineering Journal, Vol. 45, No. 4 (2003) 511–531

ANALYTICAL MODEL OF INCIPIENT BREACHING OF COASTAL BARRIERS

NICHOLAS C. KRAUS

US Army Engineer Research and Development Center,
Coastal and Hydraulics Laboratory,
3909 Halls Ferry Road, Vicksburg, MS 39180 USA
Nicholas.C.Kraus.@erdc.usace.army.mil

Received 21 September 2003
Revised 29 September 2003

A mathematical model is formulated to describe incipient breaching of coastal barrier islands. The model is based on the assumptions of idealized breach morphology and is intended to describe the growth of breaches prior to possible closure by longshore sediment transport. The two coupled, non-linear equations governing breach width and depth are solved analytically for special cases. The analytical solutions explicitly exhibit an exponential behavior in breach dimensions and reveal that the macroscale process of breach growth is controlled by seven variables: initial width and depth of the breach, equilibrium width and depth of the breach, width of the barrier island, and maximum or initial net sediment transport rates at the bottom and sides of the breach. The literature is reviewed to compile general properties of coastal breaches, and sensitivity testing shows the model to be compatible with those observations. The model is applied to simulate the 1980 breach at Moriches Inlet, New York, and reasonable agreement is found.

Keywords: Breach; inlet; barrier island; mathematical model; Moriches Inlet; morphology modeling.

1. Introduction

A coastal breach is a new opening in a narrow landmass such as a barrier island or barrier spit that allows water to flow between the water bodies on each side. Breaching is a common natural occurrence on barrier islands and spits, and at ephemeral river mouths and coastal lagoons and ponds. Breaches are also induced artificially for flood protection, to increase water quality, and as an environmental enhancement. Natural breaching can be initiated in three ways: (1) inundation from the sea combined with wave action, (2) elevated water level in the back bay or river,

causing piping and liquifaction, and (3) narrowing of a barrier island or spit by reduction of sediment supplied through longshore transport (Pierce, 1970; Kraus, Militello, and Todoroff, 2002). Coastal barrier breaching is expected to become more prevalent with rise in sea level, erosion of the coast, and continued length of service of jetties.

Once breaching occurs, tidal exchange and river discharges will typically widen the initial opening. A breach may close naturally, but, if the tidal exchange is strong and longshore sediment transport weak, it can increase in size and become a new inlet. An inlet created by breaching may compete for stability with existing inlets in the same bay system, promoting their closure. A breach adjacent to a jetty has potential for undermining and isolating the structure, and it will convey a portion of the flow that would otherwise scour the navigation channel, promoting shoaling of the channel. In addition, nearshore and beach sediment that had been protecting the structure and the shore may move through the breach and into the navigation channel, increasing dredging requirements and adding unanticipated cost to inlet entrance maintenance. A trend toward closure of an existing inlet will make the navigation channel unreliable, as well as alter the environment because of changes in water level, circulation, and salinity.

Breaches can cause loss of human life, property, infrastructure, and transportation corridors; endanger navigation and stability of adjacent inlets; and harm the environment by the exposure of bay perimeter to sea waves and by the change in bay salinity. The cost of breach closure can be high, so unintended breaches that will be a concern should be avoided by counter measures and breach contingency planning. Most breaches open rapidly and then gradually evolve over a period of weeks to months if they continue to remain open. Quantitative predictive tools are necessary to assess vulnerability of coastal barriers, design breach-prevention measures, develop breach-closure plans, estimate the fate of a breach, and evaluate the consequences of a breach to the neighboring inlets, beach, and estuarine system. Measurements and reliable predictive models of coastal breaching are lacking.

This paper introduces a mathematical model of the breaching of alluvial coastal barriers based on a macro-scale or morphologic approach. The model provides a heuristic framework for understanding the breaching process and makes apparent key dependencies that control the growth of a coastal breach.

2. Breaching Process

Review of the literature indicates that little quantitative information is available on the process of coastal barrier breaching and that predictive capability is lacking (Basco and Shin, 1999; Kraus, Militello, and Todoroff, 2002; Kraus and Wamsley, 2003). During hurricanes and storms, large numbers of ephemeral breaches can open (e.g. Texas coast, USA — Price, 1963; Hayes, 1967; and Pierce, 1970; Louisiana coast, USA — Wright, Swaye, and Coleman, 1970; and New Brunswick, Canada

— Greenwood and Keay, 1979). In a storm report documenting the damage of the September 1967 Hurricane Beulah, the US Army Engineer District, Galveston (1968) states that an inspection team found 31 breaches along 48 km of North Padre Island, Texas, barrier beach. A book edited by Leatherman (1981) collects classic, primarily descriptive papers on the processes, sedimentation, and morphology of overwash and breaching. Other papers are discussed below to supplement and update information in Leatherman (1981).

Dent (1935) documents the breaching of a 90-km long barrier beach at Ocean City, Maryland, during an August 1933 hurricane. This breach was quickly stabilized with jetties to form Ocean City Inlet and protect its federal navigation entrance channel. Terich and Komar (1974) document the breaching of Tillamook Spit, Oregon, that experienced a reduction in longshore sediment source by the construction of a jetty. At high tide, the water-filled breach at Tillamook was nearly 1.2 km wide. It was closed four years later by the construction of a setback rubble stone revetment, with a sandy beach filling the indentation.

Rice (1974) describes closure conditions for the mouth of the Russian River, California. He noted an apparent causal relation between opening of the river mouth during strong stream flow, and closure of the mouth to the season of largest waves and greatest longshore transport. Nishimura and Lau (1979) discuss possible means of minimizing closure of the mouths of small streams and propose innovative structures to promote hydraulic breaching by early-arriving storm flows as the eroding agent. Kraus, Militello, and Todoroff (2002) document breaching of a barrier spit by elevated water level in Stone Lagoon, California, and discuss the common occurrence of breaching of the Humboldt State Park, California, lagoons at the end of spring, the season of maximum precipitation. The barrier spits fully enclosing the Humboldt lagoons breach from the lagoon side when the water level rises to about 4 m above mean sea level. The lagoon breaches open to maximum dimensions within several hours, similar to dike failure, remain open at low tide for days to weeks but may be passable at high tide, then close through infilling by longshore sediment transport.

Smith and Zarillo (1988) document the growth of an artificially induced breach at Mecox Pond, Long Island, New York, that remained open during September 10–18, 1985. Mecox Pond and neighboring coastal ponds are breached by digging a channel to the Atlantic Ocean when precipitation raises the level of the ponds to threaten flooding of neighboring property. Figure 1 shows (a) the west bank of the channel, and (b) the length of a breach at Mecox Pond that was cut from a narrow pilot channel in February 1998. Steepness of the walls of the highly rectilinear breach is evident.

Terchunian and Merkert (1995) document two barrier island breaches formed at Westhampton, Long Island, New York, for which the first and initially larger breach (Fig. 2) closed by longshore transport and moderate engineering actions. A

(a) Looking west at breach cut through beach berm at Mecox Pond; Atlantic Ocean to left.

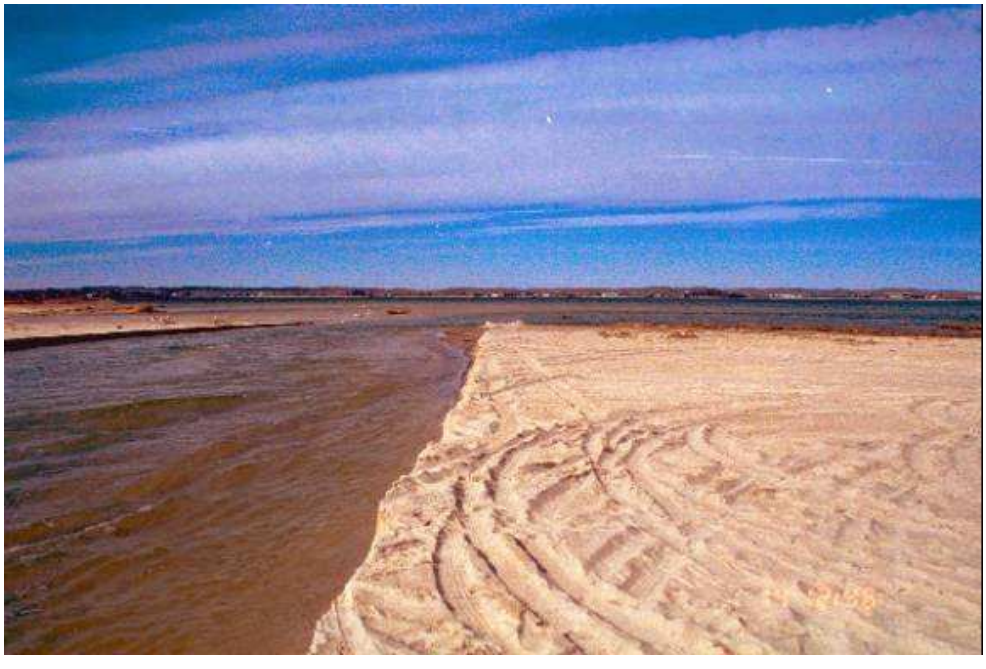

(b) Looking north from Atlantic Ocean to Mecox Pond.

Fig. 1. Mecox Pond, breached on morning of February 14, 1998; photographs taken in afternoon of February 14.

Fig. 2. Pikes Inlet, New York, December 18, 1992, about 6 days after inception of breaching.

neighboring, initially smaller breach widened because of updrift trapping of sediment by a groin field. The latter inlet, called Little Pikes Inlet, grew from approximately 30 m to 1.5 km, more than five times the width of the nearby Moriches inlet to the west that is stabilized by dual jetties.

General observations and a few case studies of breaching that occurred next to jetties have also been made, such as for the January 1980 breach at Moriches Inlet, New York (Schmeltz *et al.*, 1982; Sorensen and Smeltz, 1982) and the December 1993 breach at Grays Harbor, Washington (Arden, 2003). The breach at Grays Harbor (Fig. 3) was strongly flood dominant, typically flooding even at ebb tide. The flooding transported a large amount of sediment into the bay and navigation channel. At both sites, the breach occurred because the beach adjacent to the jetty became narrow in great part due to erosion or scalloping along the bayside intersection of the barrier island and jetty (Seabergh, 1999). Kraus and Wamsley (2003) discuss these and other locations and causes of potential breaching at other inlets stabilized by jetties in the United States.

Most detailed measurements and numerical models pertain to breaching of dikes, which differs from coastal breaching by being catastrophic and lasting on the order of hours, and by the absence longshore sediment transport that would tend to close the inlet. Visser (1998b) summarizes the literature of dike breaching in general and recent modeling (Steetzel and Visser, 1992; Visser, 1988, 1994, 1998a) and measurements (Visser, Vrijling, and Verhagen 1990; Visser *et al.* 1995; de Loof *et al.* 1996) conducted by the Dutch research community (Kraak *et al.* 1994).

Concerning predictive numerical modeling, Visser (1994, 1998) describes a five-stage two-dimensional model of sediment transport and morphology change (depth

Fig. 3. Breach at south jetty of Grays Harbor, February 1994, 2 months after inception.

and width of breach) for dike breaching that is driven by the head difference at the dike. The model was developed and verified through laboratory flume measurements and a large-scale field campaign. The model is specific to dike breaching, which appear to have different morphologic development than coastal breaching in exhibiting an irregular (humped) channel bottom and a scour hole, among other features. However, the stages of breach development and associated transport regimes identified by Visser (1994, 1998) may have general applicability. Basco and Shin (1999) present a one-dimensional (elevation) model for storm breaching. Their model, based in part on the SBEACH dune erosion model (Larson and Kraus, 1989; Larson, Kraus, and Byrnes, 1990), contains modules to erode the dune and beach across the barrier island. Hydrodynamic modules are also included to furnish wave and water-level information across the calculation domain. Sensitivity tests indicated satisfactory performance that yielded intuitively anticipated results.

From the above, the typical coastal breaching process is as follows. The initiation and course of breaching depend on the cross section of the barrier island or spit, surge hydrograph (or water level with respect to the ocean in the case of

breaching from the bay or lagoon side), presence of waves, gross longshore transport rate, hydraulic efficiency according to the location of the breach within the bay to other inlets, sedimentary composition of the site, and presence of barriers such as a jetties, groins, and headlands. In the absence of erosion-resistant boundaries, coastal breaches appear to open rapidly, then gradually widen and deepen to some equilibrium dimensions. The rapid-growth stage is referred here as incipient breaching, occurring prior to strong influence of longshore sediment transport. Ephemeral breaches tend to open widely and deepen only to about mean sea level, whereas breaches that become more permanent tend to increase in depth to that of neighboring natural inlets or to depths of neighboring inlets before stabilization. If a breach tends to become stable, known empirical relations for tidal inlets would then govern the morphology (see Kraus, 2001 for a summary).

Breaching occurs at lower areas in the coastal barrier, and the side slopes of the initial breach tend to be steep, being eroded by strong flow, notching, and collapse in a type of avalanching. If erosion-resistant materials are not present, a breach typically widens and deepens rapidly to approach equilibrium dimensions that depend on the factors described above. Models of coastal breaching are still at a rudimentary stage. The model formulated here is based on observations of general tendencies of breaches.

3. Analytical Model of Incipient Breaching

A breach through a barrier is idealized as shown in the rectangular section in Fig. 4. To derive a closed-form solution, the governing equations describing breaching are

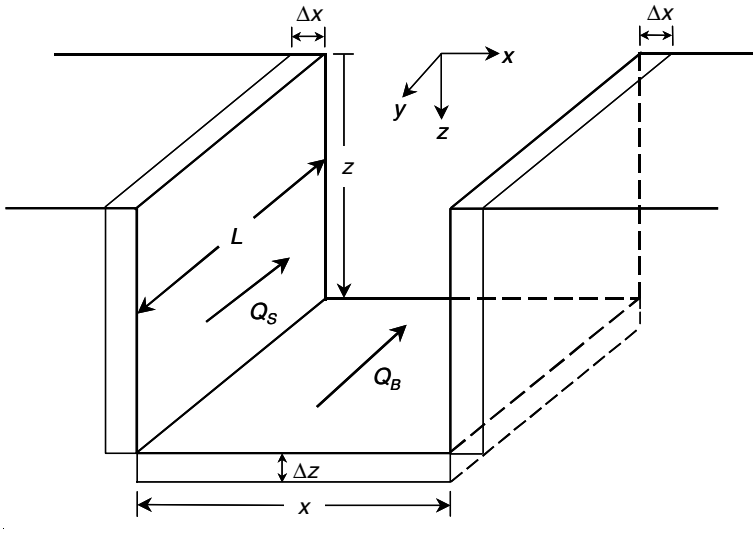

Fig. 4. Definition sketch for breaching model.

developed under the assumptions that: (a) sediment (sand) volume is conserved; (b) the initial condition is known, (c) sediment transport can occur at the bottom of the breach and at its sides; (d) the breach will approach equilibrium if external forces do not intervene; and (e) longshore sediment transport is weak or can be neglected. Assumptions (b) to (e) can be relaxed in extension of the present analytic model or in a numerical model. Assumption (e), weak longshore transport relative to the breaching process, limits this model to describing incipient breaching. Tanaka, Takahashi, and Takahashi (1996) and Kraus (1998) present analytical models of river mouth and inlet cross-sectional areas formed under a balance of tidal action that includes river discharge and longshore transport under waves. Those analytical models that relate to the equilibrium condition of an inlet or river mouth would be a next logical stage of the present model development.

Under the stated assumptions and by reference to Fig. 4, conservation of mass yields the following equations,

$$Lz\Delta x = \hat{Q}_S \Delta t \tag{1}$$

for breach width, and,

$$Lx\Delta z = \hat{Q}_B \Delta t \tag{2}$$

for breach depth, where L is length of the breach through the coastal barrier, z and x are depth and width of the breach, respectively, t is time, and $\hat{Q}_S$ and $\hat{Q}_B$ are net transport rates along the sides (assumed to be equal on each side) and bottom of the breach, respectively. In general, the sediment transport rates $\hat{Q}_S$ and $\hat{Q}_B$ are functions of the acting hydrodynamic forces and breach configuration.

To proceed with an analytic solution, transport by surge, or by flood or ebb tide is not distinguished in forming the net transport rate in a morphologic representation, and the following functional relations are taken:

$$\hat{Q}_S = Q_S \left(1 - \frac{x}{x_e}\right), \quad \hat{Q}_B = Q_B \left(1 - \frac{z}{z_e}\right) \tag{3}$$

where Q_S and Q_B are constant maximum transport rates that are not necessarily equal, and x_e and z_e are values of the breach width and depth, respectively, if the breach achieved equilibrium. The morphologic parameterization of the transport rates by Eq. (3) makes them time dependent, with the net transport rates going to zero as equilibrium is approached. The equilibrium values x_e and z_e could be specified in at least three ways, as through: (1) experience with previous breaches at or near the study site, (2) specification via an empirical formula such as given by Mehta (1976), Graham and Mehta (1981), and Shigemura (1981), or (3) through operation of a hydrodynamic model, by which the critical shear stress or similar diagnostic quantity indicating cessation of transport can be calculated. The morphologic approach as taken in forming Eq. (3) is discussed by Kraus (2001) as a

means of assuring robust results though imposition of morphologic constraints — in this situation, of equilibrium values.

Insertion of Eq. (3) into Eqs. (1) and (2) and taking the limit yields the following coupled, first-order nonlinear governing equations for breaching:

$$\frac{dx}{dt} = \frac{a}{z}\left(1 - \frac{x}{x_e}\right), \quad a = \frac{Q_S}{L}, \quad x(0) = x_0 > 0 \tag{4}$$

and

$$\frac{dz}{dt} = \frac{b}{x}\left(1 - \frac{z}{z_e}\right), \quad b = \frac{Q_B}{L}, \quad z(0) = z_0 > 0 \tag{5}$$

Equations (4) and (5) cannot be solved without specifying a non-zero perturbation of the barrier (representing an indentation or "pilot channel" through the barrier), as given by a finite initial width x_0 and initial depth z_0. Equation (4) describes a one-sided breach such as constrained by a jetty in nature or a wall in a flume. If both sides of the breach can move, then the value of Q_S in Eq. (4) should be doubled.

3.1. *Solution for x_e and $z_e \to \infty$*

This special case corresponds to very short elapsed time of incipient breaching, for which the governing Eqs. (4) and (5) reduce to $dx/dt = a/z$ and $dz/dt = b/x$. The solution of this simplified set of coupled non-linear equations is,

$$x = \left[x_0^{\frac{a+b}{a}} + (a+b)\frac{x_0^{b/a}}{z_0} t \right]^{\frac{a}{a+b}} \tag{6}$$

and

$$z = \left[z_0^{\frac{a+b}{b}} + (a+b)\frac{z_0^{a/b}}{x_0} t \right]^{\frac{b}{a+b}} \tag{7}$$

If the initial perturbation or pilot channel is small, the cross-sectional area of the breach is found to grow as

$$xy \sim (a+b)t = \frac{Q_S + Q_B}{L} t \tag{8}$$

indicating a linear increase in area immediately after the breach occurs. For the special case of $a = b$, Eqs. (6) and (7) simplify to,

$$x = \left(x_0^2 + 2a\frac{x_0}{z_0} t \right)^{1/2} \tag{9}$$

and

$$z = \left(z_0^2 + 2a\frac{z_0}{x_0} t \right)^{1/2} \tag{10}$$

which, for a small initial perturbation, yields $xy \sim 2at$, a special case of Eq. (8). Equations (9) and (10) make apparent the significant role the dimensions of the initial perturbation take on the course of breach development. Although Eqs. (6)–(10) govern incipient breaching, they have limited value in being restricted to very short elapsed time. More informative solutions are obtained by solving Eqs. (4) and (5), which incorporate modification and control of breach growth by the inclusion of equilibrium.

3.2. *Solution with equilibrium*

Closed-form solution of Eqs. (4) and (5) is not found feasible for arbitrary values of the factors a and b, but, for the situation of $a = b$ (signifying $Q_S = Q_B = Q$), the following solution emerges:

$$x = x_e(1 - f(x)\mathrm{e}^{-t/\tau}) \tag{11}$$

and

$$z = z_e(1 - g(z)\mathrm{e}^{-t/\tau}) \tag{12}$$

in which,

$$\tau = \frac{V_e}{Q} \tag{13}$$

where $V_e = x_e z_e L$ is the volume of the breach at equilibrium, and

$$f(x) = \left(1 - \frac{x_0}{x_e}\right)\left(\frac{1 - \alpha x/x_e}{1 - \alpha x_0/x_e}\right)^{1/\alpha} \tag{14}$$

$$\alpha = \frac{x_0/x_e - z_0/z_e}{(1 - z_0/z_e)x_0/x_e} \tag{15}$$

$$g(z) = \left(1 - \frac{z_0}{z_e}\right)\left(\frac{1 - \beta z/z_e}{1 - \beta z_0/z_e}\right)^{1/\beta} \tag{16}$$

$$\beta = \frac{z_0/z_e - x_0/x_e}{(1 - x_0/x_e)z_0/z_e} \tag{17}$$

Iteration is required to evaluate Eqs. (11) and (12) because of the appearance of the dependent values in Eqs. (14) and (16). Equations (4) and (5) can also be solved numerically, as through a Runge-Kutta procedure, and this was done to confirm the validity of the closed-form solutions above, as well as to perform calculations for $a \neq b$.

In addition to making basic dependencies of breach growth explicit, Eqs. (11) and (12) provide closed-form solutions with which to check numerical solutions of the simultaneous, non-linear governing Eqs. (4) and (5). This simple morphologic model

indicates that breach growth is controlled by seven parameters: x_0, z_0, x_e, z_e, Q_S, Q_B, and L. Equations (11)–(17) reveal morphologic functional dependencies that describe the approach of a breach toward equilibrium. The quantity $\tau = x_e z_e L/Q$ is a characteristic morphologic time scale governing growth toward equilibrium for a given maximum net transport rate of sediment removed from the breach. The dimensions of the initial perturbation or pilot channel of the barrier island exert great control on the time development of the breach and whether it will tend to widen more than deepen at a greater rate, or vice versa, prior to approaching equilibrium width and depth. Such properties of the solution are explored in the next section.

Equations (11) and (12) indicate an exponential growth of a breach toward equilibrium, giving a more rapid growth initially, followed by gradual increase in depth and width to equilibrium. The time behavior of the morphologic model qualitatively describes the growth of breaches observed in nature and in the laboratory, whether induced by storm surge or by a difference in water level on the sides of the barrier island.

The volume of the breach is $V = xzL$, with x and z given by numerical solution of Eqs. (4) and (5), respectively, for a general situation, or by Eqs. (11) and (12) for the special case $Q_S = Q_B$. The depth of the breach is measured from the top of the barrier island in the morphologic breach model. For stable inlets, empirical formulas are available for estimating channel cross-sectional area (e.g. Jarrett (1976) for large tidal inlets; Byrne, Gammish, and Thomas (1980) for small tidal inlets). The depth corresponding to this channel cross-sectional area is measured from mean sea level to the bottom of the breach and not from the top of barrier island. Therefore, in applications of predictive expressions for equilibrium breach area $x_e z_e$, one must account for the distance from the top of the barrier island to the elevation of mean sea level.

3.3. *Sensitivity tests of morphologic breach model*

Equations (4) and (5) were solved numerically for general cases, after first confirming the numerical solution with the analytical solution given by Eqs. (11) and (12). Figures 5–7 plot calculations for $Q_S = 500$ m^3/day, $Q_B = 1,000$ m^3/day, $L = 300$ m, and equilibrium width $x_e = 300$ m, and equilibrium depth $z_e = 5$ m. These values are considered representative of the many small breaches along the Texas and Louisiana coasts, as determined in the literature review. Note that if the crest of the barrier island lies, for example, 3 m above mean sea level, then the depth of the breach below mean sea level is 2 meters. For these calculations, the width of the pilot channel or low section in the barrier was specified as $x_0 = 10$ m, correspondingly, say, to walkway or blowout through the dunes, and results were plotted for initial depths $z_0 = 0.1$, 1, 2, and 3 m. Plots are normalized by the corresponding equilibrium value. Volume of the breach is predicted to be relatively insensitive to initial breach depth

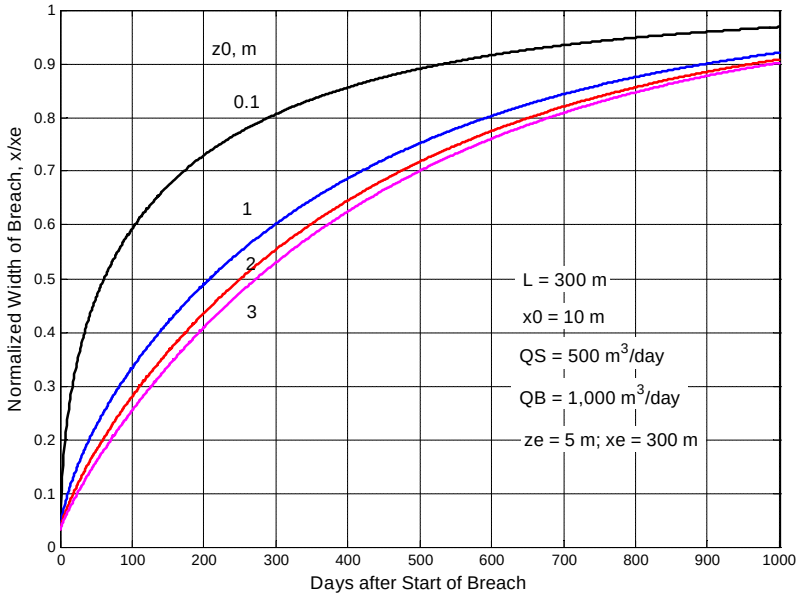

Fig. 5. Solution of Eq. 4 for breach width, different values of initial breach depth.

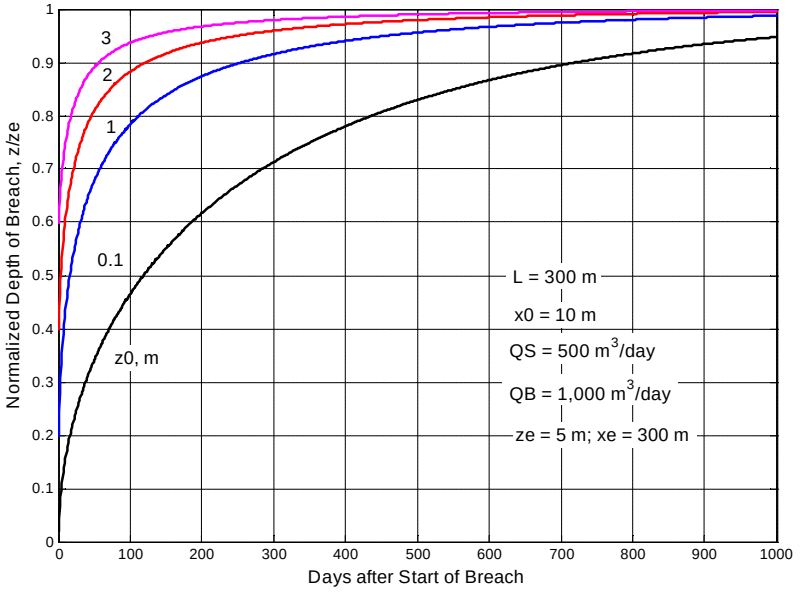

Fig. 6. Solution of Eq. 5 for breach depth, different values of initial breach depth.

(Fig. 7). Growth in volume toward equilibrium starts faster for larger initial depth, but then the curves cross at about 30 days elapsed time. The volume then grows slightly faster for smaller initial depth because of the larger value of the transport rate at the bottom than on the side.

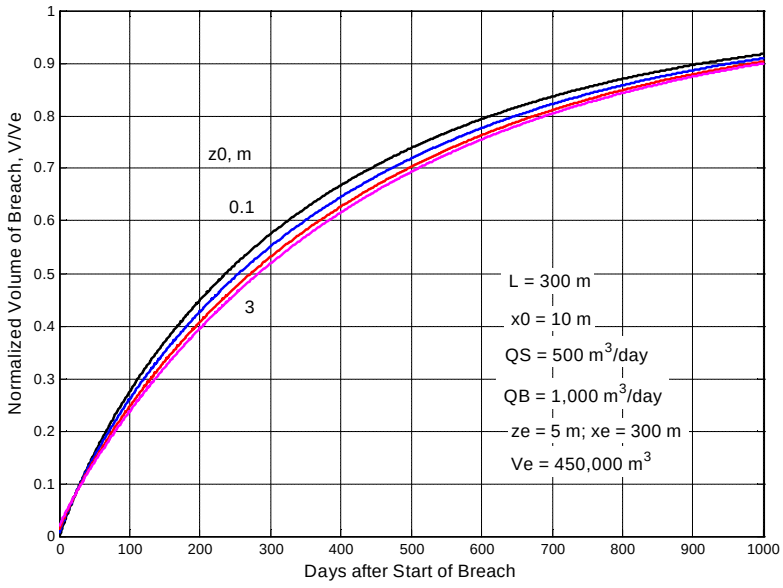

Fig. 7. Growth of breach volume for fixed initial width and different initial depths corresponding to Figs. 5 and 6.

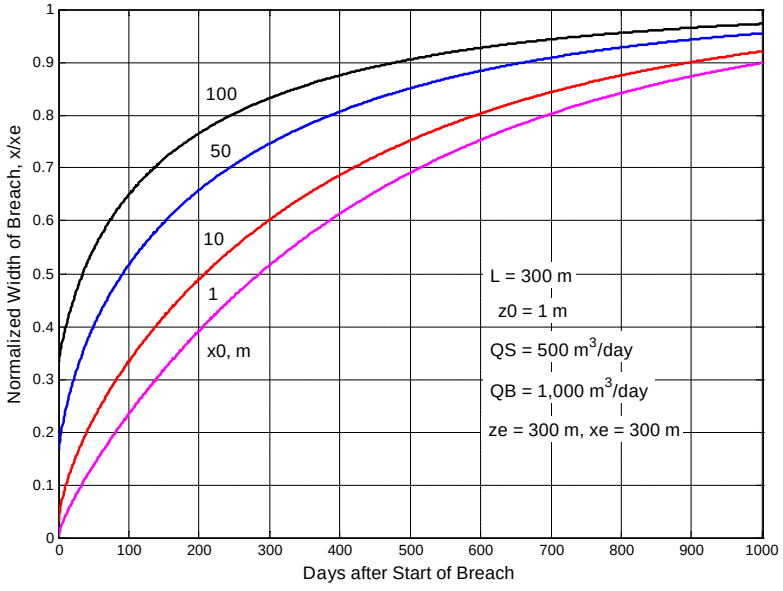

Fig. 8. Solution of Eq. (4) for breach width, different values of initial breach width.

The morphologic model predicts that breach width grows faster for smaller initial depth. Of course, breach depth approaches equilibrium faster for greater initial depth. Growth of the dimensions of a breach depends directly on the transport rates Q_S and Q_B, and so general conclusions cannot be made. However, if these rates are

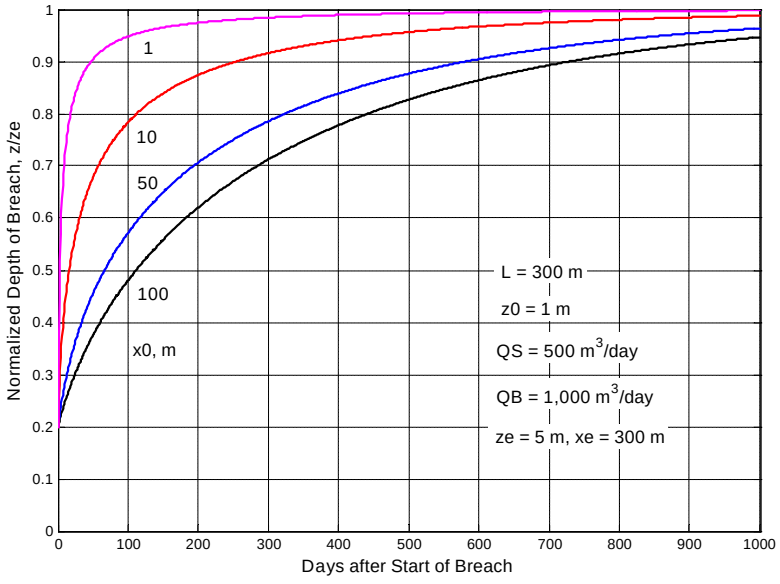

Fig. 9. Solution of Eq. (5) for breach depth, different values of initial breach width.

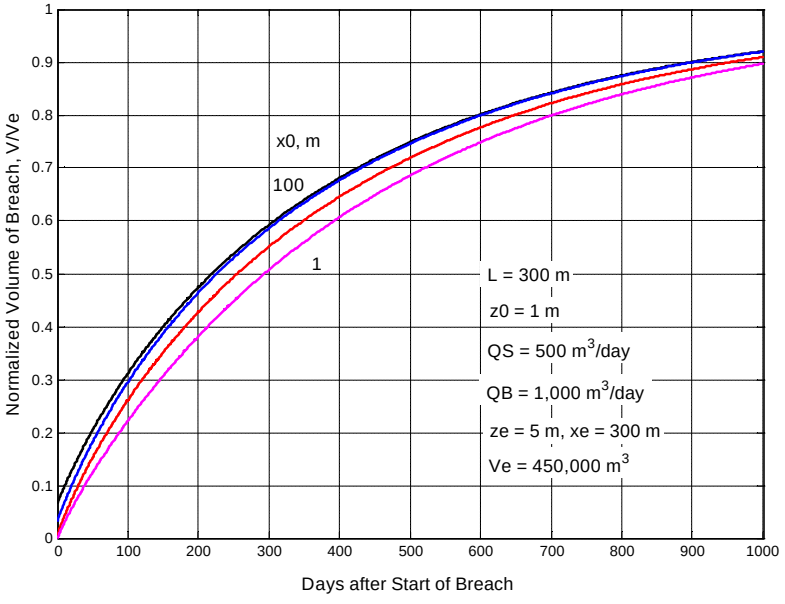

Fig. 10. Growth of breach volume for fixed initial depth and different initial widths corresponding to Figs. 8 and 9.

of comparable magnitude, as taken here, then the trends shown are qualitatively correct.

Similar calculations are shown in Figs. 8–10 for fixed initial depth $z_0 = 1$ m and initial widths $x_0 = 1$, 10, 50, and 100 m. As expected, breach width approaches

equilibrium faster for larger initial width, whereas breach depth approaches equilibrium faster for small initial width. The volume of the breach approaches equilibrium faster for larger initial width both because of the large initial width and because $Q_B > Q_S$ in this example.

4. Simulation for 1980 Breach at Moriches Inlet, New York

Moriches Inlet is a federally maintained entrance located on the eastern shore of Long Island, New York, connecting Moriches Bay (part of the large Great South Bay) to the Atlantic Ocean (Fig. 11). Without stabilization by structures, inlet channels on eastern Long Island meander and have maximum depth of about 3 m with respect to mean lower low water. The ocean mean tide range at Moriches Inlet is about 1 m. Moriches Inlet has a well-documented history of opening and closing in the past century (Czerniak, 1977; Schmeltz *et al.*, 1982). The modern inlet was opened by a storm in 1953 during construction of dual jetties that are spaced 245 m apart.

After inlet opening in 1953, the barrier island on the eastern (updrift) side of Moriches Inlet gradually narrowed, primarily due to erosion at the jetty and shoreline intersection on the back bay. Sorensen and Schmeltz (1982) indicate the adjacent beach to have been about 100 m wide in 1972 (taken to be L in the simulations described below). A storm occurring on January 14–16, 1980 created a breach at the narrowest point in the barrier island, about 300 m east of the east jetty. By May 1980, the breach had enlarged to reach the jetty and grow to approximately 885 m width according to an October observation (see Fig. 12 for a September

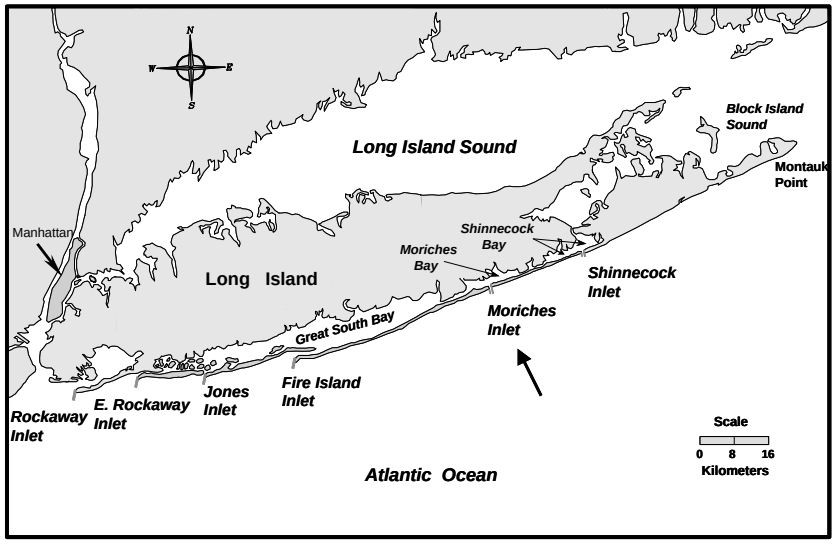

Fig. 11. Location map for Moriches Inlet, Long Island, New York.

Fig. 12. Breach at Moriches Inlet, New York, September 21, 1980. Photograph taken 9 months after the January 1980 breach. Note east jetty became isolated from land because of the breach.

Table 1. Dimensions of 1980 breach at Moriches Inlet, New York (data from Schmeltz *et al.*, 1982, and Sorenson and Schmeltz, 1982).

Date, 1980	Estimated Elapsed Time, Days	Breach Width, m	Breach Depth from Assumed Elevation of Barrier Island Crest, m
15 January	0	30 (assumed here for x_0)	1 (assumed here for z_0)
16 January	1	90	3.6
20 January	5	215	4
"May"	90	885	7

observation), more than three times the width between the two jetties, and with a depth of 3 m relative to mean low water (Sorensen and Schmeltz, 1982).

Table 1 compiles available information about the breach dimensions. For the tabulation, it was assumed that the mean elevation of the barrier island was 3 m above mean low water. This value was added to the depths of the breach reported by Sorensen and Schmeltz (1982). In addition, an initial width of 30 m and initial depth (local lowering in the barrier island) of 1 m were assumed for application of the breach morphology model. Based on additional photographic evidence, it was concluded for this analysis that near-maximum width had been achieved sometime before the May observation. This value was set in the model at 90 days elapsed time after opening of the breach. Construction began in October 1980 to close the

breach, for which 900,000 m^3 were dredged from the bay and trucked from a quarry in equal amounts. This volume provides a check for the model.

The breach morphology model was established for the area with the initial dimensions as in Table 1. Trial and error readily gave a visual good fit to the data with base rates of $Q_S = Q_B = 30,000$ m^3/day for the maximum transport rates at the inception of breaching. Such rates are well within the daily production capacity of, for example, 0.5- and 0.6-m (20- and 24-inch) diameter dredges operating in shallow water (Turner, 1996) and, therefore, are considered readily attainable by storm surge combined with tidal exchange. To explore sensitivity of the model to variations in maximum transport rates, the base rates were multiplied by 2 and 0.5 to define plausible upper and lower bounds, respectively. Figures 13–15 plot calculations with the observed width, depth, and estimated volume of the breach, and the results with upper and lower limits of assumed maximum transport are depicted with dashed lines. The volume at different times was estimated from the dimensions as given in Table 1 and the reported fill volume, assumed to occupy the same approximate equilibrium volume in May.

The breach morphology model captures the qualitative behavior of the breach evolution, with rapid initial growth followed by gradual approach to equilibrium. Width, depth, and volume of the breach are in quantitative agreement with observations for all available data points through time. Calculations with the lower estimate of the maximum transport rate deviate more from the observations than

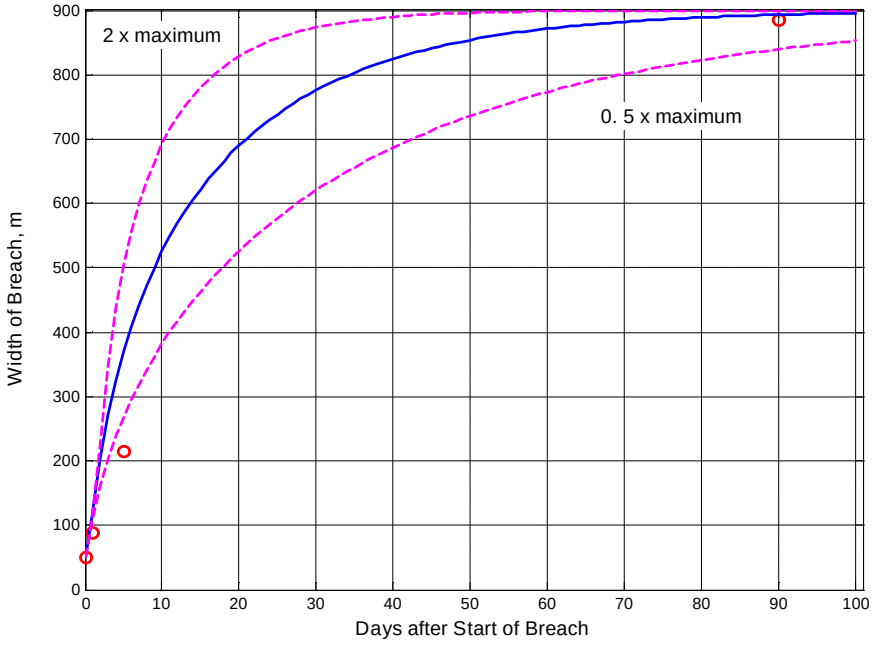

Fig. 13. Simulation of growth of breach width, Moriches Inlet.

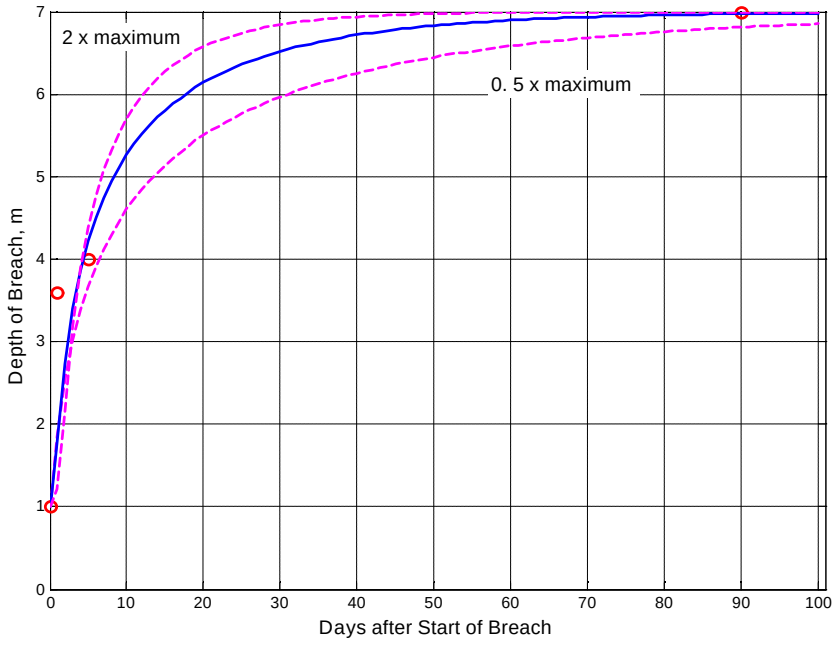

Fig. 14. Simulation of growth of breach depth, Moriches Inlet.

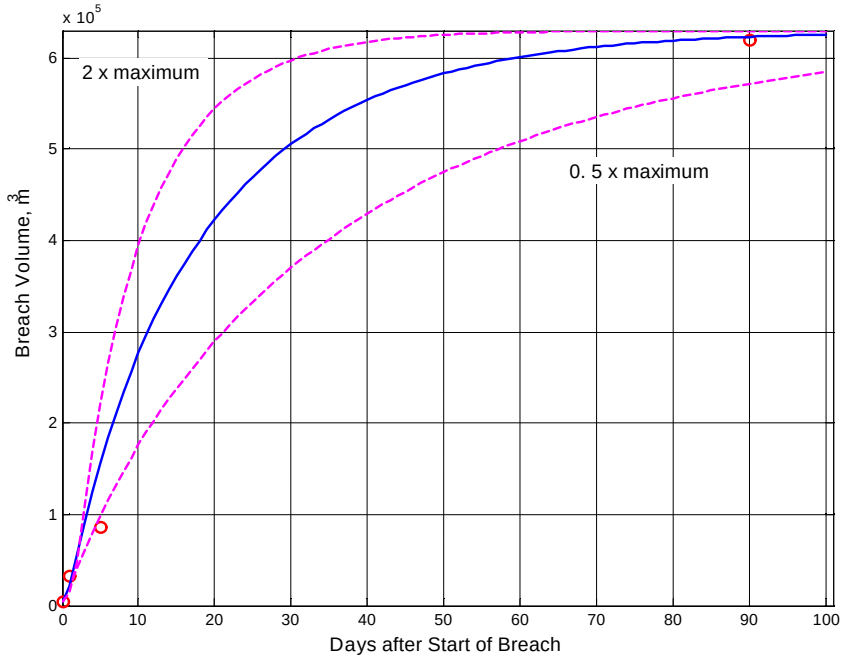

Fig. 15. Simulation of growth of breach volume, Moriches Inlet.

those for the base rate and double the base rate. The characteristic morphology growth time is $\tau = V_e/Q = 900,000/30,000 = 30$ days.

5. Discussion and Conclusions

This paper has presented an analytical morphologic model of incipient breaching of alluvial barriers. Closed-form solutions were obtained through simplifying assumptions about breach configuration and approach to equilibrium. Processes associated with the driving hydrodynamics of sediment transport and bank erosion and collapse are represented implicitly through specification of the maximum sediment transport rates at the bed and the sides of the breach at initial breaching, and by the equilibrium values of the breach width and depth. Additional or microscale physical processes could be represented in numerical solution of the governing Eqs. (4) and (5), for which time-dependent sediment transport rates and bank failure could be calculated while maintaining a known, geometry. Seven variables are found to control breach growth in such a macroscale description: initial width and depth of the breach, equilibrium width and depth of the breach, width of the barrier island, and maximum or initial net sediment transport rates at the bottom and sides of the breach. Breach growth follows an exponential behavior governed by a characteristic time scale $\tau = V_e/Q$, where V_e is the volume of the breach at equilibrium, and Q is a representative maximum net sediment transport rate through the breach.

Sensitivity testing of the morphologic model and comparison with observations of the 1980 breach at Moriches Inlet, New York, demonstrated validity of the model in capturing the general qualitative and quantitative features of coastal barrier breaching. Data-based refinements can be made by the inclusion of empirical predictive formulas for the equilibrium depth and width. Most of these extensions would require information on the hydrodynamics and sediment transport at the breach, which would need to be supplied by hydrodynamic and sediment transport models coupled to the morphologic breaching model. However, estimates of the basic governing variables drawn from engineering judgment and observations at the site and at nearby inlets may be suitable for obtaining a reconnaissance-level prediction of coastal breach growth without recourse to sophisticated models.

Acknowledgements

This study was conducted under the Inlet Geomorphology and Channels Work Unit of the Coastal Inlets Research Program (CIRP), US Army Corps of Engineers (USACE). Review by colleagues Ty Wamsley and William Seabergh are appreciated. Permission was granted by Headquarters, USACE, to publish this information.

References

Arden, H. T. (2003). South jetty breach fill at Grays Harbor, Washington, Doing the right thing with dredged material, *Shore & Beach* **71**, 1, pp. 3–5.

Basco, D. R. and Shin, C. S. (1999). A one-dimensional numerical model for storm-breaching of barrier islands, *J. Coastal Res.* **15**, 1, pp. 241–260.

Byrne, R. J., Gammish, R. A. and Thomas, G. R. (1980). Tidal prism-inlet area relations for small tidal inlets, *Proc. 17th Coastal Eng. Conf.*, ASCE, pp. 2,517–2,533.

Czerniak, M. T. (1977). Inlet interaction and stability theory verification, *Proc. Coastal Sediments '77*, ASCE, pp. 754–773.

De Looff, H., Steetzel, H. J. and Kraak, A. W. (1996). Breach growth: Experiments and modelling, *Proc. 25th Coastal Eng. Conf.*, ASCE, pp. 2,746–2,755.

Dent, E. J. (1935). Establishing a permanent inlet at Ocean City, Maryland, *Shore and Beach* **3**, 3, pp. 89–94.

Graham, D. S. and Mehta, A. J. (1981). Burial design criteria for tidal flow crossing, *Trans. Eng. J.* **107**, TE2, pp. 227–242.

Greenwood, B. and Keay, P. A. (1979). Morphology and dynamics of a barrier breach: A study in instability, *Canadian J. Earth Sciences* **16**, 8, pp. 1, 533–1, 546.

Hayes, M. O. (1967). Hurricanes as geological agents, south Texas coast, *American Assoc. Petroleum Geologists Bull.* **51**: 937–942.

Jarrett, J. T. (1976). Tidal prism-inlet area relationships, GITI Report 3, US Army Corps of Engineers, Waterways Experiment Station, Vicksburg, MS.

Kraak, A. W., Bakker, W. T., van de Graaff, J., Steetzel, H. J. and Visser, P. J. (1994). Breach-growth research programme and its place in damage assessment for a polder, *Proc. 24th Coastal Eng. Conf.*, ASCE, pp. 2,197–2,206.

Kraus, N. C. (2001). On equilibrium properties in predictive modeling of coastal morphology change, *Proc. Coastal Dynamics 01*, ASCE, pp. 1–15.

Kraus, N. C., Militello, A. and Todoroff, G. (2002). Barrier breaching processes and barrier spit breach, Stone Lagoon, California, *Shore & Beach* **70**, 4, pp. 21–28.

Kraus, N. C. and Wamsley, T. V. (2003). Coastal barrier breaching, Part 1: Overview of breaching processes, ERDC/CHL CHETN IV-56, US Army Engineer Research and Development Center, Vicksburg, MS, http://chl.wes.army.mil/library/publications/chetn.

Larson, M., and Kraus, N. C. (1989). SBEACH: Numerical model for simulating storm-induced beach change, Report 1: Empirical foundation and model development, Technical Report CERC-89-9, US Army Engineer Waterways Experiment Station, Vicksburg, MS.

Larson, M., Kraus, N. C., and Byrnes, M. R. (1990). SBEACH: Numerical model for simulating storm-induced beach change, Report 2: Numerical formulation and model tests, Technical Report CERC-89-9, US Army Engineer Waterways Experiment Station, Vicksburg, MS.

Leatherman, S. P. (ed). (1981). *Overwash Processes*, Benchmark Papers in Geology, Hutchison Ross Pub. Co., Stroudsberg, PA, **58**, 376 pp.

Mehta, A. J. (1976). Stability of some New Zealand coastal inlets, Letter to the Editor, *NZJ. Marine and Freshwater Res.* **10**, 4, pp. 737–740.

Nishimura, J. K. and Lau, L. S. (1979). Structure for automatic opening of closed stream mouths, *Shore & Beach* **47**, 4, pp. 3–8.

Pierce, J. W. (1970). Tidal inlets and washover fans, *J. Geol.* **78**: 230–234.

Price, W. A. (1963). Patterns of flow and channeling in tidal inlets, *J. Sedimentary Petrology* **33**: pp. 279–290.

Rice, M. P. (1974). Closure conditions mouth of the Russian River, *Shore and Beach* **42**, 1, pp. 15–20.

Schmeltz, E. J., Sorensen, R. M., McCarthy, M. J. and Nersesian, G. (1982). Beach/inlet interaction at Moriches Inlet, *Proc. 18th Coastal Eng. Conf.*, ASCE, pp. 1,062–1,077.

Seabergh, W. C. (1999). Inner-bank erosion at jetty-shoreline intersection, *Proc. Coastal Sediments '99*, ASCE, pp. 2235–2248.

Shigemura, T. (1981). Tidal prism-throat width relationships of the bays of Japan, *Shore & Beach* **49**, 3, pp. 34–39.

Smith, G. L. and Zarillo, G. A. (1988). Short-term interactions between hydraulics and morphodynamics of a small tidal inlet, Long Island, New York, *J. Coastal Res.* **4**: 301–314.

Sorensen, R. M. and Schmeltz, E. J. (1982). Closure of the breach at Moriches Inlet, *Shore & Beach* **50**, 4, pp. 22–40.

Steetzel, H. J. and Visser, P. J. (1992). Profile development of dunes due to overflow, *Proc. 23rd Coastal Eng. Conf.*, ASCE, pp. 2,669–2,679.

Tanaka, H., Takahashi, R. and Takahashi, A. (1996). Complete closure of the Nanakita River Mouth in 1994, *Proc. 26th Coastal Eng. Conf.*, ASCE, pp. 4,545–4,556.

Terchunian, A. V. and Merkert, C. L. (1995). Little Pikes Inlet, Long Island, New York, *J. Coastal Res.* **11**, 3, pp. 697–703.

Terich, T. A. and Komar, P. D. (1974). Bayocean Spit, Oregon — History of development and erosional destruction, *Shore & Beach* **42**, 2, pp. 3–10.

Turner, T. M. (1996). *Fundamentals of Hydraulic Dredging*, 2nd edn., ASCE Press, New York, 258 pp.

US Army Engineer District, Galveston (1968). Report on Hurricane "Beulah," Storm Report, US Army Corps of Engineers, Galveston, Texas.

Visser, P. J. (1988). A model for breach growth in a dike-burst, *Proc. 21st Coastal Eng. Conf.*, ASCE, 1,897-1910.

Visser, P. J., Vrijling, J. K. and Verhagen, H. J. (1990). A field experiment on breach growth in sand-dikes, *Proc. 22nd Coastal Eng. Conf.*, ASCE, pp. 2,087–2,100.

Visser, P. J. (1994). A model for breach growth in sand-dikes, *Proc. 24th Coastal Eng. Conf.*, ASCE, pp. 2,755–2,769.

Visser, P. J., *et al.* (1995). A large-scale experiment on breaching in sand-dikes, *Proc. Coastal Dynamics '95*, ASCE, pp. 583–594.

Visser, P. J. (1998a). Breach erosion of sand dikes, *Proc. 26th Coastal Eng. Conf.*, ASCE, pp. 3,516–3,528.

Visser, P. J. (1998b). Breach growth in sand-dikes, Report No. 98–1, Hydraulic and Geotechnical Engineering Divison, Delft University of Technology, 172 pp.

Wright, L. D., Swaye, F. J. and Coleman, J. M. (1970). Effects of Hurricane Camille on the landscape of the Breton-Chandeleur Chain and the eastern portion of the Lower Mississippi Delta, Technical Report 76, Coastal Studies Institute, Louisiana State University, Baton Rouge, LA, 32 pp.